

Impedance spectroscopy study of $\text{Nd}_2\text{NiO}_{4+\delta}$, LSM and platinum electrodes by micro-contact technique

F. Mauvy*, C. Lalanne, S. Fourcade, J.M. Bassat, J.C. Grenier

Institut de Chimie de la Matière Condensée de Bordeaux (ICMCB-CNRS), Université de Bordeaux I, Av. Schweitzer, 33608 Pessac Cedex, France

Available online 21 March 2007

Abstract

The impedance spectra of $\text{Nd}_2\text{NiO}_{4+\delta}$, $\text{La}_{1-x}\text{Sr}_x\text{MnO}_3$ and platinum pin-shaped electrodes pressed on the surface of an electrolyte pellet (Yttria Stabilized Zirconia) have been recorded as a function of temperature, in air atmosphere, under zero dc conditions. Such an electrode configuration was used to study the characteristics of the air electrode reaction with respect to the nature of the electrode material, the geometry of the electrode–electrolyte contact being the same for all electrodes. The impedance data were analyzed and the results evidence different oxygen reduction mechanisms depending on the nature of the oxide, Mixed Ionic and Electronic Conducting (MIEC) oxide for the nickelate, bad ionic but electronic conductor for the manganite and metallic for the platinum.

© 2007 Elsevier Ltd. All rights reserved.

Keywords: Fuel cells; Transition metal oxides; Impedance

1. Introduction

Nowadays the strontium-doped lanthanum manganite is a well established cathode material in the commercial Solid Oxide Fuel Cells (SOFC) currently under development. However, various laboratories, mostly motivated by the goal of lowering the operating cell temperature, have proposed alternative materials as mixed ionic and electronic conducting (MIEC) oxides.^{1,2} Then, a question can be addressed: how to compare their cathodic performances? In this scope, it is needed to study the oxygen reduction mechanism from an electrochemical point of view. It is easy to measure their electronic conductivities under air, versus temperature, using the four probe technique. Concerning the ionic transport properties, the oxygen diffusion coefficient can be measured using for example the isotopic exchange technique provided that the measurements are carried out on highly densified ceramics.³ Another important feature is the electrocatalytic activity of the different electrode materials. For example, the surface exchange coefficient even measured on a compact sample depends significantly on its surface state. Furthermore, the fairly wide diversity of the performance characteristics reported for the conventional electrodes clearly shows

that, beside the intrinsic properties of the electrode materials, the electrode process and the microstructure are also determining parameters. Under these circumstances, any attempt to classify electrode materials should imply an appropriate normalization based on clear assumptions regarding the extent of the electrode reaction zone.

In terms of reaction mechanisms, two types of electrodes are consensually distinguished⁴:

- Triple Phase Boundary (TPB) electrodes for which the electroactive species are supplied to the reaction zone by surface diffusion. This case concerns the metallic electrodes and the electronic and poor ionic conducting oxides.⁵
- Internal Diffusion (ID) electrodes which are characterized by an oxygen ion supply to the electrode interface through a bulk diffusion in the electrode material. This is the case of the MIEC oxides.

In this study, we carried out experiments using sharp micro-electrodes, the aim being to better understand the oxygen reduction mechanism at the solid electrolyte/cathode interface and to measure electrochemical parameters which can be normalized with respect to their real active surface area, independently on the electrode microstructure.⁶ Using such electrodes has been previously reported by Kleitz,⁷ Mogensen,⁸ Tunold⁹ and their collaborators.

* Corresponding author. Tel.: +33 540002517; fax: +33 540008373.
E-mail address: mauvy@icmcb-bordeaux.cnrs.fr (F. Mauvy).

The SOFC cathode materials used for the micro-electrodes are the MIEC oxides $\text{Nd}_2\text{NiO}_{4+\delta}$ and the classical perovskite $\text{La}_{0.8}\text{Sr}_{0.2}\text{MnO}_3$ which is a very bad ionic conducting oxide. A platinum probe was also studied as a reference for comparison. The aim is to compare the electrochemical properties of these materials under air, the yttria stabilised zirconia (YSZ) being the electrolyte.

2. Experimental procedure

2.1. Preparation of the materials and pointed micro-electrodes

Commercial submicronic powders were used for electrolyte material (YSZ powder (8 mol% Y_2O_3) from Tosoh Co. Ltd.) and lanthanum strontium manganite cathode (LSM powder (20% strontium) from Nextech Materials Co. Ltd.).

The neodymium nickelate oxide $\text{Nd}_2\text{NiO}_{4+\delta}$ was prepared using the nitrate–citrate route from stoichiometric amounts of Nd_2O_3 (Strem) and NiO (Aldrich) dissolved in nitric acid. After addition of citric acid, the solution was dehydrated at 120°C and slowly heated until self-combustion of the precipitates. They were finally fired for 8 h in the temperature range $950\text{--}1080^\circ\text{C}$.

Pellets (20 mm in diameter and 1–2 mm thick) were then sintered in air, at 1350°C , for 2 h, which led to relative densities higher than 95%. Then, they were cut in bar form and pointed micro-electrodes were machined like a cone tip using diamond tools. An example is reported in Fig. 1. The contact radius and the electrode contact surface area were estimated after experimental series of optical and electronic micrographs of the cone tips.

The micro-electrodes (tips of the cathode materials) were pressed into contact with the surface of the YSZ pellet by a spring.

2.2. Impedance spectroscopy measurements

The impedance diagrams were obtained from an Autolab Frequency Response Analyzer PGSTAT 30. The signal amplitude

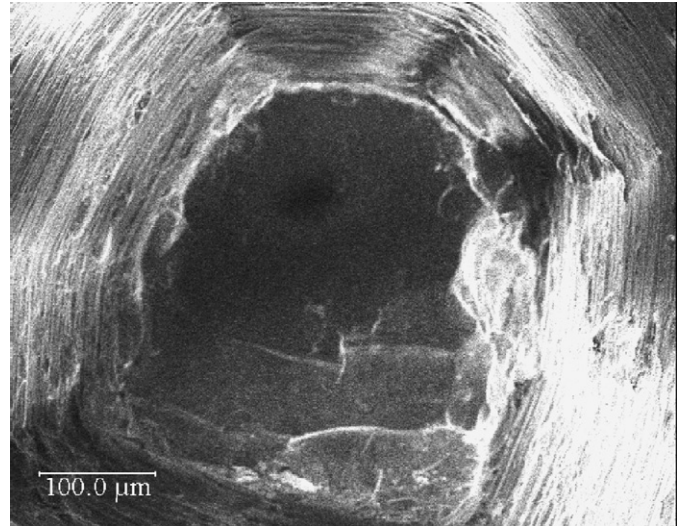


Fig. 1. Photograph of a $\text{Nd}_2\text{NiO}_{4+\delta}$ tip (taken from the end of the tip).

was 50 mV and a 0 mV dc bias was used. When required, a curve fitting was performed using the Zview software. Typical examples of Nyquist diagrams measured under air, at 550°C are reported in Fig. 2.

Most of the impedance diagrams recorded in this study can be decomposed, in the frequency range 1 MHz to 0.01 Hz, into two or three loops, namely LF (for low frequencies), MF (for middle frequencies) and HF (for high frequencies).

3. Results and discussion

3.1. Relaxation frequencies

A methodology based on the relaxation frequencies of the different contributions has been used for the identification of the different contributions observed in the spectra.¹⁰

Generally, a diagram showing simultaneously all the contributions is not observable over the whole temperature range and loop overlaps are usually present. Fig. 3 shows the Arrhenius plots of the relaxation frequencies measured with

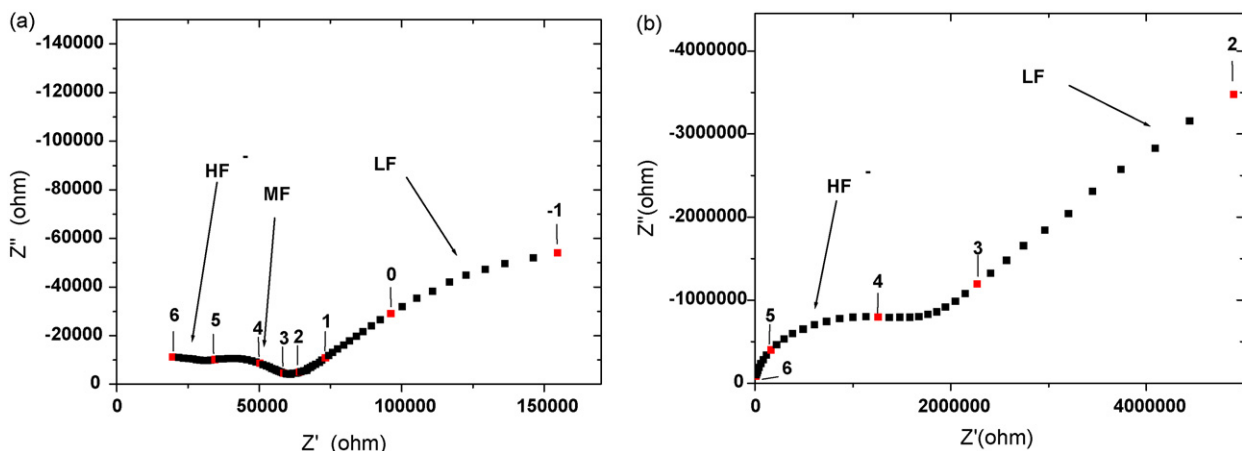


Fig. 2. Typical impedance diagrams at 550°C under air (the numbers indicate the decimal log of the signal frequencies). (a) Tip: $\text{Nd}_2\text{NiO}_{4+\delta}$, pellet: YSZ; (b) tip: LSM, pellet: YSZ.

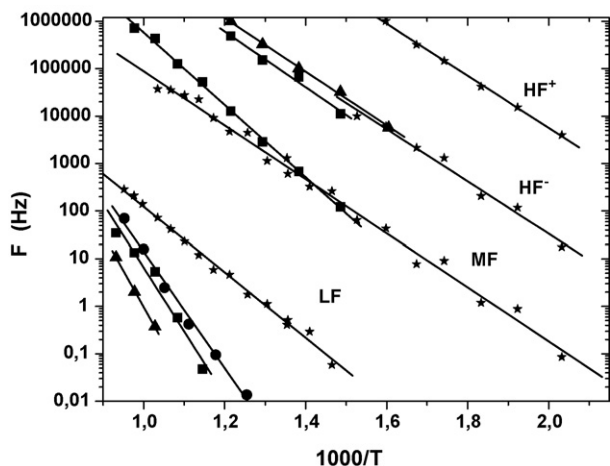


Fig. 3. Arrhenius plots of the relaxation frequencies measured with the micro-contacts $\text{Nd}_2\text{NiO}_{4+\delta}/\text{YSZ}$ (■) and LSM/YSZ (▲) and Pt/YSZ (●) half-cells. Results obtained with a symmetrical cell $\text{Nd}_2\text{NiO}_{4+\delta}/\text{YSZ}/\text{Nd}_2\text{NiO}_{4+\delta}$ (porous electrodes) are also reported (★).

half-cells made of YSZ pellets and micro-electrodes of the MIEC $\text{Nd}_2\text{NiO}_{4+\delta}$ oxide, metallic LSM oxide and Pt, respectively. Results previously obtained with $\text{Nd}_2\text{NiO}_{4+\delta}$ porous electrodes are also reported.¹⁰

According to these graphs, four different domains of relaxation frequencies can be observed: HF^+ and HF^- , MF and LF. On the basis of previous works on porous electrodes,¹⁰ the HF^+ impedance contribution is attributed to YSZ bulk properties and the HF^- one to YSZ grain boundary properties. On the other hand, the MF and LF contributions are more difficult to assign because they are not well separated depending on the electrode material. Generally, the MF contribution is assigned to the oxygen transfer at the electrode–electrolyte interface and the low frequency contribution to the electrode processes (oxygen adsorption/diffusion).

In the case of $\text{Nd}_2\text{NiO}_{4+\delta}$ tip, both oxygen charge transfer and mass transfer are well deconvoluted whereas it is not true for LSM tip.

At this stage, the active surface area for the oxygen reduction reaction should be discussed. When a MIEC oxide is used, the reaction can take place all over the whole sample surface whereas, when the electrode is a metal, the oxygen reduction is localized at the molecular oxygen–metal–electrolyte triple contact. Therefore one may conclude that the oxygen transfer at the nickelate oxide/YSZ micro-contact should not be a limiting step to be taken into account in the mechanism of the oxygen reduction.

Concerning the LSM micro-electrode, no MF contribution is observed, even over a large temperature range (Fig. 3) and the LF contribution can only be fitted at high temperature because of the important impedance values. These results show that in the case of dense metallic-like micro-contacts, the electrode processes are limiting steps for oxygen reduction, which is in agreement with measurements previously observed on LSM electrodes.⁴ Similar conclusions can be drawn for the platinum metal micro-electrodes. Therefore, both can be considered as pure TPB electrodes.

3.2. Resistive and capacitive contributions

The R_{HF} resistance values deduced from the high frequencies depressed semi circle (or by extrapolation to high frequencies) are attributed to the electrolyte resistance. We have observed a small dispersion of the values which can be assigned to small differences in the pin shapes. Nevertheless, the activation energy values (≈ 1.0 eV) deduced from the resistance Arrhenius plots well agree with the literature data¹⁰ relative to the conductivity σ measured with pellet and large platinum electrodes.

Applying the Newman's relation, the contact surface area between the working electrode and the electrolyte can be determined, assuming that the electrode is a disk of radius r , according to the following relation: $r = (4\sigma R_{\text{HF}})^{-1}$, the high frequencies resistance R_{HF} being the electrolyte resistance, and σ the electrolyte conductivity value taken from the literature. The contact surface areas of the pin electrodes (S) were then calculated and found close 0.01 mm^2 , in agreement with the evaluation made from the microscopic observations.

In Fig. 4 are reported the area specific resistance (ASR) values calculated from the polarization resistance $R_{\text{P}} = R_{\text{MF}} + R_{\text{LF}}$ (where $R_{\text{MF}} + R_{\text{LF}}$ are the Middle frequencies and Low Frequencies resistances respectively) and $\text{ASR} = (R_{\text{P}} S)/2$. For the MIEC nickelate oxide, the R_{P} values are systematically lower than those of LSM, which confirms the interest of this type of materials for SOFC applications. Actually, LSM (as well as platinum) electrodes show very important polarization resistances that can be measured, on this type of micro-electrodes, only at temperatures higher than 700°C , R_{P} being only the LF impedance contribution. Finally, the important values of the LF resistive contribution confirm the “bad MIEC” behaviour of LSM electrode and allows us to classified this material in TPB electrode–type family whereas the nickelate material shows quite different electrochemical behaviour (especially in the MF range). These results are in agreement with the ID electrode concept for the MIEC cathodes.

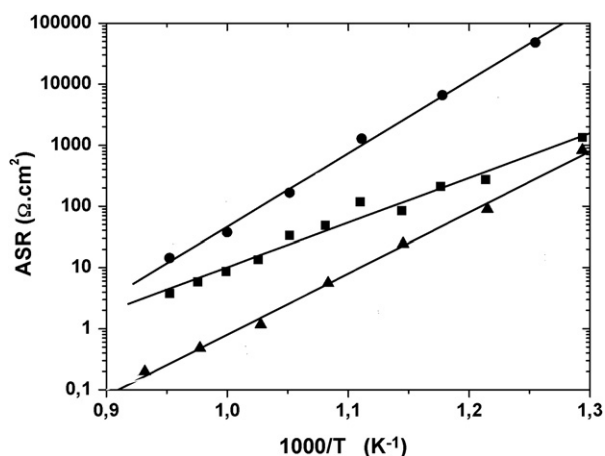


Fig. 4. Arrhenius plots of the ASR associated to the electrode contributions for $\text{Nd}_2\text{NiO}_{4+\delta}$ (▲), LSM (■) and Pt (●) electrodes in contact with YSZ pellets.

4. Conclusion

Impedance spectroscopy measurements have been performed on $\text{Nd}_2\text{NiO}_{4+\delta}/\text{YSZ}$, $\text{La}_{0.8}\text{Sr}_{0.2}\text{MnO}_3/\text{YSZ}$ and Pt/YSZ micro-contact electrodes and it has been noticed that the impedance spectra of the samples are significantly different. The difference in behaviour of $\text{Nd}_2\text{NiO}_{4+\delta}$ and LSM has been assigned to the transport properties of these two materials. As reported in the literature, the fact that LSM is essentially electronic conductor whereas the nickelate is a mixed ionic and electronic conductor likely explain the difference between the two cathode behaviours, the reason being that the reduction kinetics is favoured on the $\text{Nd}_2\text{NiO}_{4+\delta}$ compound as observed on porous electrodes. This conclusion is corroborated by the behaviour of the metallic platinum micro-electrode that is quite similar to that of LSM.

References

1. Zipprich, W. and Wiemhöfer, H.-D., *Solid State Ionics*, 2000, **135**, 699–707.

2. Mauvy, F., Bassat, J.-M., Boehm, E., Manaud, J.-P., Dordor, P. and Grenier, J.-C., *Solid State Ionics*, 2003, **158**, 17–28.
3. Boehm, E., Bassat, J. M., Dordor, P., Mauvy, F. and Grenier, J. C., *Solid State Sci.*, 2003, **5**, 973–981.
4. Siebert, E., Hammouche, A. and Kleitz, M., *Electrochem. Acta*, 1995, **40**(11), 1741–1753.
5. Mitterdorfer, A. and Gauckler, L. J., *Solid State Ionics*, 1999, **117**, 187–202.
6. Fleig, J., *Solid State Ionics*, 2003, **161**, 279–289.
7. Baker, R., Guindet, J. and Kleitz, M., *J. Electrochem. Soc.*, 1997, **144**, 2427.
8. Juhl, M., Mogensen, M., Jacobsen, T., Zachau-Christiansen, B., Thorup, N. and Skou, E., In *Solid Oxide Fuel Cells IV, PV95-1. The Electrochemical Society Proceedings Series*, ed. M. Dokiya, O. Yamamoto, H. Tagawa and S. C. Singhal, 1995, p. 554.
9. Jerdal, L. O., Tunold, R., Thorup, N. and Mogensen, M., In *1st Europ. SOFC Forum*, ed. B. Thortensen. U. Bossel, Oberrohrdorf, Switzerland, 1994, p. 745.
10. Mauvy, F., Lalanne, C., Bassat, J.-M., Grenier, J.-C., Zhao, H., Huo, L. and Stevens, P., *J. Electrochem. Soc.*, 2006, **153**(8), A1547–A1553.